Subfertility and defective folliculogenesis in female mice lacking androgen receptor

Yueh-Chiang Hu*†, Peng-Hui Wang*†‡, Shuyuan Yeh*, Ruey-Sheng Wang*§, Chao Xie*, Qingquan Xu*, Xinchang Zhou*, Hsiang-Tai Chao‡, Meng-Yin Tsai¶, and Chawnshang Chang*‖

*George Whipple Laboratory for Cancer Research, Departments of Pathology and Urology, University of Rochester, Rochester, NY 14642; ‡Department of Obstetrics and Gynecology, Taipei Veterans General Hospital and National Yang-Ming University, Taipei 112, Taiwan; §Department of Obstetrics and Gynecology, Taipei Medical University, Taipei 110, Taiwan; and ¶Reproductive Medicine Institute, Chang Gung University, Kaohsiung 833, Taiwan

Communicated by Henry Lardy, University of Wisconsin, Madison, WI, June 18, 2004 (received for review August 16, 2003)

The roles of the androgen receptor (AR) in female fertility and ovarian function remain largely unknown. Here we report on the generation of female mice lacking AR ($AR^{-/-}$) and the resulting influences on the reproductive system. Female $AR^{-/-}$ mice appear normal but show longer estrous cycles and reduced fertility. The ovaries from sexually mature $AR^{-/-}$ females exhibited a marked reduction in the number of corpora lutea. After superovulation treatment, the $AR^{-/-}$ ovaries produced fewer oocytes and also showed fewer corpora lutea. During the periovulatory period, an intensive granulosa apoptosis event occurs in the $AR^{-/-}$ preovulatory follicles, concurrent with the down-regulation of p21 and progesterone receptor expression. Furthermore, the defective conformation of the cumulus cell–oocyte complex from the $AR^{-/-}$ females implies a lower fertilization capability of the $AR^{-/-}$ oocytes. In addition to insufficient progesterone production, the diminished endometrial growth in uteri in response to exogenous gonadotropins indicates that $AR^{-/-}$ females exhibit a luteal phase defect. Taken together, these data provide *in vivo* evidence showing that AR plays an important role in female reproduction.

The androgen receptor (AR) exerts its biological function through activation of target gene expression via a sequence of processes, including ligand binding, homodimerization, nuclear translocation, DNA binding, and complex formation with coregulators and general transcription factors (1–3). While the AR has long been known to play a central role in the development of male sex organs, secondary sexual characteristics, and the initiation and progression of prostate cancer (4–6), its physiological roles in females remain unclear. To this end, we recently generated female AR knockout ($AR^{-/-}$) mice and demonstrated that the loss of AR retards mammary gland development (7). Also, the study of $AR^{-/-}$ MCF-7 breast cancer cells has indicated the requirement of AR in breast cancer growth (7).

Ovarian folliculogenesis is a process of the follicular development starting from the smallest primordial follicles recruited into the growth pool through primary, preantral, and antral stages to the largest Graafian or preovulatory follicles (POFs) that ovulate in response to the luteinizing hormone (LH) surge. After ovulation, the remaining granulosa cells and theca cells within the POFs differentiate into luteal cells to form the corpus luteum (CL) (8). However, in each cycle, only one or very few of the primordial follicles initially recruited are destined to become POFs; most of them undergo apoptotic death (atresia), mainly at the early antral stage (9). Follicle-stimulating hormone (FSH) is the major survival factor that rescues the early antral follicles from atresia (9). The entire folliculogenesis process involves a complex network of paracrine, autocrine, and endocrine signals, including sex hormones, in a stage-dependent manner. The AR is present in the ovary in almost all stages of folliculogenesis and has been suggested to play a proliferative role for follicular development (10, 11). In addition, androgen treatment induces the expression of insulin-like growth factor-I and insulin-like growth factor-I receptors and enhances the growth of the immature follicles in the primate ovary (12). Androgen treatment also augments the granulosa cell responsiveness to FSH, resulting in an enhancement of follicular proliferation (13). In contrast, many other reports indicate that androgen/AR can inhibit follicular development by increasing follicular atresia (14, 15). This discrepancy is partly attributed to lack of animal models to unravel the physiological roles of the AR in females. Because the AR gene is located on the X chromosome and males lacking functional AR are infertile, homozygous female offspring lacking functional AR cannot be generated. In this study, we overcame this difficulty by using the Cre-lox conditional knockout strategy (7) to generate the female mice lacking functional AR, and we characterized the *in vivo* roles of the AR in the female reproductive system.

Materials and Methods

Generation of Female $AR^{-/-}$ Mice. Animal care, construction of the targeting vectors, and the strategy of generation of $AR^{-/-}$ females are described in refs. 7 and 16. Briefly, male mice carrying floxed *AR* on the X chromosome (fAR/Y) were mated with females genotyped with *AR*/*ar* ACTB-Cre to produce female $AR^{-/-}$ mice carrying the genotype *ar*/*ar* ACTB-Cre. ACTB-Cre is a transgene containing the β-actin promoter to drive Cre recombinase cDNA expression that excises the floxed *AR* fragment (entire exon 2) on the genome. Genotyping was performed by using PCR on the genomic DNA isolated from the tails of 3-week-old mice, as described in refs. 7 and 16, and was confirmed by RT-PCR on the RNAs extracted from ovaries and uteri. The primers used were 5′-AATGGGACCTTGGATGGAGAAC-3′ and 5′-TCCCTGCTTCATAACATTTCCG-3′, as illustrated in Fig. 1*A*.

Fertility of Female $AR^{-/-}$ Mice. Ten- to 11-week-old female $AR^{+/+}$, $AR^{+/-}$, and $AR^{-/-}$ mice ($n = 8$ for each genotype) were subjected to a continuous mating study. Two female mice were housed with one 8- to 10-week-old known fertile male mouse, and male mice were rotated weekly. Cages were monitored daily, and the number of pups and litters was recorded.

Superovulation and Oocyte Count. Superovulation was carried out on female $AR^{+/+}$, $AR^{+/-}$, and $AR^{-/-}$ mice at the ages indicated in the figures. The protocol consisted of a single i.p. injection with 5 units of pregnant mare serum gonadotropin (PMSG) (Sigma) for 48 h, followed by 5 units of human chorionic gonadotropin (hCG) (Sigma) for an additional 18 h or indicated times. The animals were then killed and the genital tracts were excised for histological examination or RNA extraction. The oocyte/cumulus masses were surgically harvested from the oviducts and cultured in Dulbecco's modified Eagle's medium (Invitrogen) supplemented with 20% FCS and antibiotics. After treating with 0.3% hyaluronidase

Abbreviations: AR, androgen receptor; CL, corpus luteum; COC, cumulus cell–oocyte complex; hCG, human chorionic gonadotropin; FSH, follicle-stimulating hormone; FSHR, FSH receptor; LH, luteinizing hormone; PMSG, pregnant mare serum gonadotropin; POF, preovulatory follicle; TUNEL, terminal deoxynucleotidyltransferase-mediated dUTP nick end labeling.

†Y.-C.H. and P.-H.W. contributed equally to this work.

‖To whom correspondence should be addressed. E-mail: chang@urmc.rochester.edu.

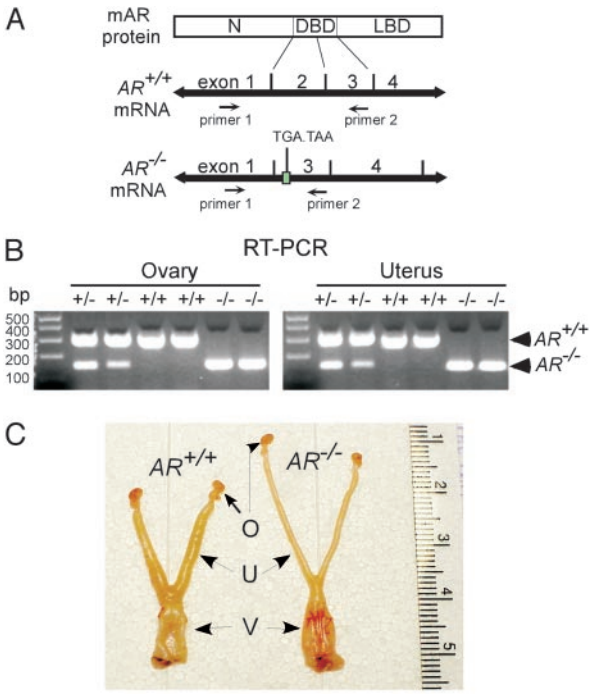

Fig. 1. RT-PCR analysis of AR transcripts and macroscopic comparison of the reproductive organs of female $AR^{+/+}$ and $AR^{-/-}$ mice. (*A*) Schematic diagram of the primer design that distinguishes $AR^{-/-}$ from $AR^{+/+}$ transcripts. The size of RT-PCR products from $AR^{+/+}$ and $AR^{-/-}$ mRNAs is 305 and 153 bp, respectively. The splicing of exon 1 and 3 in $AR^{-/-}$ mRNA causes a translational frameshift, and two additional stop codons occur within exon 3. N, N-terminal domain; DBD, DNA-binding domain; LBD, ligand-binding domain. (*B*) The RT-PCR analyses revealed that ovaries and uteri from $AR^{-/-}$ females carried the exon 2-deleted transcripts. (*C*) The genital tracts of 8-week-old $AR^{+/+}$ and $AR^{-/-}$ females at the estrus stage were compared. The estrus stages of the mice were determined by vaginal smears that showed hundreds of cornified cells. $AR^{+/+}$ uteri are wider and thicker than $AR^{-/-}$ uteri. O, ovary; U, uterus; V, vagina.

(Sigma) for 10 min, oocytes surrounded with and not surrounded with cumulus cells were categorized and counted.

Histology. For each female mouse, one ovary was processed for hematoxylin and eosin staining, and the other one was subjected to real-time RT-PCR. Tissues were fixed in 4% paraformaldehyde at 4°C overnight and then paraffin-embedded for further study. The number of follicles for each ovary was counted from at least five of the largest sections and was normalized by the total ovarian area in the section (15). The ovary area was measured with PHOTOSHOP Version 6.0 (Adobe Systems, San Jose, CA). The follicle types, including primordial, preantral, antral, atretic follicles, and CLs, were classified as described in ref. 15. Data were presented as mean ± SD from at least two pairs of mice. For cell apoptosis detection, the Fluorescent FragEL DNA fragmentation kit (EMD Bioscience, San Diego) was used on the tissue sections, as instructed by the manufacturer. Photomicroscopy was performed by using a Nikon Eclipse E800 system.

Results

RT-PCR Analysis of the Targeted *AR* Gene. By using a Cre-lox conditional knockout strategy, we targeted *AR* exon 2, which encodes the first zinc finger of the DNA-binding domain, to generate a female mouse lacking functional AR. This deletion caused a translational frameshift in AR mRNA by means of the splicing of exon 1 and exon 3 transcripts, resulting in the creation of two stop codons at new amino acid positions 533 and 534, which are located within the exon 3 (Fig. 1*A*). To confirm that ovaries and uteri from female $AR^{-/-}$ mice produce the targeted transcripts, we performed RT-PCR analyses, which revealed that RNAs from those organs completely lacked the *AR* exon 2 and were 153 bp in length, as compared with 305 bp in length for their $AR^{+/+}$ counterparts, when we used a pair of primers located on *AR* exon 1 and exon 3, respectively (Fig. 1*B*).

Genital Tract Phenotype of $AR^{-/-}$ Females. Next, we examined the reproductive organs from age-matched female mice. Under macroscopic examination, the $AR^{-/-}$ reproductive system appeared normal; however, when we compared the genital tracts from 8-week-old sexually mature $AR^{+/+}$ and $AR^{-/-}$ females at the estrus stage, $AR^{+/+}$ uteri transformed to the receptive status and exhibited obvious thick uterine walls, whereas $AR^{-/-}$ uteri exhibited less response to ovulation and remained thin (Fig. 1*C*). The difference was more significant between 16-week-old $AR^{+/+}$ and $AR^{-/-}$ female mice (data not shown). To determine whether this defective uterine response to ovulation in $AR^{-/-}$ mice affects their reproduction, we examined the pregnant uteri of female $AR^{+/+}$ and $AR^{-/-}$ mice and found that pregnant $AR^{-/-}$ mice bore fewer embryos (5.3 ± 1.5) than $AR^{+/+}$ mice (9.8 ± 2.2), suggesting that $AR^{-/-}$ females have reduced fertility.

Subfertility of Female $AR^{-/-}$ Mice. To further evaluate the reproductive performance of female $AR^{-/-}$ mice, we conducted a continuous mating study using sexually mature female mice ($n = 8$ for each genotype) at 10 to 11 weeks of age mating with known fertile male mice. After 12 weeks of mating, female $AR^{-/-}$ mice consistently exhibited reduced fertility by showing a significant decrease of litter size (4.5 ± 2.5 pups per litter, $P < 0.0001$) compared with either $AR^{+/+}$ or $AR^{+/-}$ females, at 9.8 ± 2.5 and 8.0 ± 2.4 pups per litter, respectively (Table 1). Nevertheless, female $AR^{-/-}$ mice had an average of 2.3 ± 0.7 litters in a 12-week period, which was also significantly lower than $AR^{+/+}$ or $AR^{+/-}$ females, which had 3.3 ± 0.5 and 3.1 ± 0.8 litters per female, respectively (Table 1). To determine whether the reduced litter number in $AR^{-/-}$ females involves an abnormal estrous cycle, vaginal smears were taken daily from four $AR^{+/+}$ and three $AR^{-/-}$ mice at 10 weeks of age for one month. We found that the $AR^{+/+}$ mice reached metestrus every 7.1 ± 1.6 days, whereas the $AR^{-/-}$ mice had longer estrous cycles, reaching metestrus every 11.0 ± 2.7 days. We consistently observed that $AR^{-/-}$ females had a longer diestrus (6.3 ± 1.5 days) compared with $AR^{+/+}$ mice (2.3 ± 1.3 days). Therefore, the longer estrous cycle in $AR^{-/-}$ mice may contribute to the reduced litter numbers observed in the continuous mating test (Table 1). Note that the mice studied were group-housed. It is known that group-housed mice have longer estrous cycles than individually housed ones [e.g., 6.18 ± 0.66 days vs. 4.75 ± 0.21 days (18)]. In addition, although female mice may vary in duration of reproductive life (19), we found that a few female $AR^{-/-}$ mice were infertile at 5–6 months of age. In contrast, all $AR^{+/+}$ females were still fertile at these ages.

To further assess the ovarian function of the $AR^{-/-}$ female mice, we induced superovulation with exogenous gonadotropins in immature $AR^{+/+}$, $AR^{+/-}$, and $AR^{-/-}$ female mice at 25 days of age to determine the oocyte production per female. The results from 12 mice ($n = 4$ for each genotype) indicate that female $AR^{-/-}$ mice

Table 1. Fertility tests of *AR* mutant females

Genotype	*n*	Litters	Pups	Pups per litter	Litters per female
$AR^{+/+}$	8	26	255	9.8 ± 2.5	3.3 ± 0.5
$AR^{+/-}$	8	25	201	8.0 ± 2.4*	3.1 ± 0.8
$AR^{-/-}$	8	18	81	4.5 ± 2.5‡	2.3 ± 0.7§

Known fertile males were bred with 10- to 11-week-old female liittermates for 12 weeks. Results are presented as mean ± SD. *, $P = 0.012$ vs. $AR^{+/+}$, Student's unpaired *t* test; ‡, $P < 0.0001$ vs. $AR^{+/+}$, Student's unpaired *t* test; §, $P = 0.0058$ vs. $AR^{+/+}$, Student's unpaired *t* test.

Table 2. Oocytes produced from female mice after superovulation

Genotype	Cumulus cells	Oocyte count	
		Mean ± SD	Range
$AR^{+/+}$	Surrounded	20.3 ± 5.6	13–26
	Dissociated	6.3 ± 3.4	3–11
	Total	26.5 ± 7.9	16–34
$AR^{+/-}$	Surrounded	17.5 ± 1.9	15–19
	Dissociated	8.0 ± 3.4	4–12
	Total	25.5 ± 4.9	19–31
$AR^{-/-}$*	Surrounded	10.5 ± 5.6	5–18
	Dissociated	5.8 ± 3.0	2–9
	Total	16.3 ± 8.2*	7–27

Female mice ($n = 4$ for each genotype) at age 25 days were subjected to superovulation treatment. Oocyte/cumulus masses were then surgically extracted from their oviducts, and oocytes surrounded with or not surrounded with cumulus cells were counted after hyaluronidase digestion for 10 min. Results are presented as mean ± SD. *, $P < 0.05$ vs. $AR^{+/+}$, Student's unpaired *t* test.

produced fewer oocytes (16.3 ± 8.2) compared with female $AR^{+/+}$ and $AR^{+/-}$ mice (26.5 ± 7.9 and 25.5 ± 4.9, respectively) (Table 2), indicating that the function of the $AR^{-/-}$ ovary is defective *per se*, which would contribute to the reduced fertility of the $AR^{-/-}$ females, as shown in Table 1. In addition, we also observed that the structure of the cumulus cell–oocyte complex (COC) from $AR^{-/-}$ mice was less condensed and less intact than that from $AR^{+/+}$ and $AR^{+/-}$ mice under microscopy (data not shown). Accordingly, after 0.3% hyaluronidase treatment, the disassociation of the oocytes from the surrounding cumulus cells occurred more quickly in $AR^{-/-}$ COCs (35.6% disassociation in 10 min; 5.8 ± 3.0 from a total of 16.3 ± 8.2) than in $AR^{+/+}$ COCs (23.8% disassociation in 10 min; 6.3 ± 3.4 from a total of 26.5 ± 7.9) (Table 2). Thus, the defective conformation of the COC may suggest a lower fertilization capability of $AR^{-/-}$ oocytes, compared with their $AR^{+/+}$ counterparts.

Morphology of the $AR^{-/-}$ Ovaries. Ovaries of $AR^{+/+}$ and $AR^{-/-}$ mice ($n = 2$ for each genotype) at 4 weeks of age were compared. There was no significant difference in the number of growing follicles (Fig. 2*A* and *B*). When comparing follicle numbers in $AR^{-/-}$ and $AR^{+/+}$ ovaries, there were 5.3 ± 2.2 vs. 6.5 ± 0.8 per mm^2 antral follicles and 4.1 ± 1.0 vs. 4.3 ± 1.8 per mm^2 preantral follicles. No CL could be identified at this age (Fig. 2*C*).

At 16 weeks of age, the most striking difference between $AR^{+/+}$ and $AR^{-/-}$ mice was that $AR^{-/-}$ ovaries showed apparently fewer CLs (Fig. 2 *D* and *E*). The statistical analyses also indicate a significant difference in the number of CLs in $AR^{-/-}$ (0.24 ± 0.17 per mm^2) and $AR^{+/+}$ (2.93 ± 0.74 per mm^2) mice ($P < 0.001$; Fig. 2*F*). A locally very thin granulosa layer in large, growing antral follicles in the $AR^{-/-}$ ovary (Fig. 2*E*, open arrowhead) could be observed, as compared with the even thickness of the granulosa layer in the $AR^{+/+}$ ovary (Fig. 2*D*, arrows), suggesting that there are insufficient granulosa cells during follicle growth in the $AR^{-/-}$ ovary, which may contribute to the impairment of CL formation.

Morphology of the Superovulated $AR^{-/-}$ Ovaries. To gain further insight into the reduced fertility, the superovulated ovaries from 4.5-week-old $AR^{+/+}$ and $AR^{-/-}$ mice ($n = 5$ for each genotype) were histologically compared. After superovulation, the $AR^{-/-}$ ovaries exhibit significantly fewer and smaller CL formations compared with their $AR^{-/-}$ counterparts (Fig. 3 *A–C*), similar to the defects in the 16-week-old $AR^{-/-}$ females (Fig. 2 *D–F*). The finding of reduced CL formation in $AR^{-/-}$ ovaries was further supported by the quantitative analysis of the functional markers for luteinization (8). That is, the expression levels of p27 and side-chain cleavage cytochrome P450 were reduced, and the expression of cytochrome P450 17α enzyme was increased in $AR^{-/-}$ ovaries (Fig. 3*D*). P450 aromatase was not affected at this stage (Fig. 3*D*). In addition, the granulosa cells were largely reduced in number and were disorganized in the large antral follicle of $AR^{-/-}$ ovaries (Fig. 3*F*) compared with their $AR^{+/+}$ counterparts (Fig. 3*E*), although the oocyte seemed healthy, with no sign of apoptosis. Interestingly, the cumulus cells were mostly disassociated from the oocyte during ovulation in some of the $AR^{-/-}$ POFs (Fig. 3*G*), suggesting that the development of the COC is abnormal, possibly because of the loss of granulosa cells. This result is consistent with the finding that the conformation of $AR^{-/-}$ COCs was less condensed (Table 2). In addition, 22 h after hCG injection, the granulosa cells in the $AR^{+/+}$ POFs differentiated into large luteal cells (Fig. 3*H*) and underwent luteolysis, with cell apoptosis occurring in the later stage of lutein-

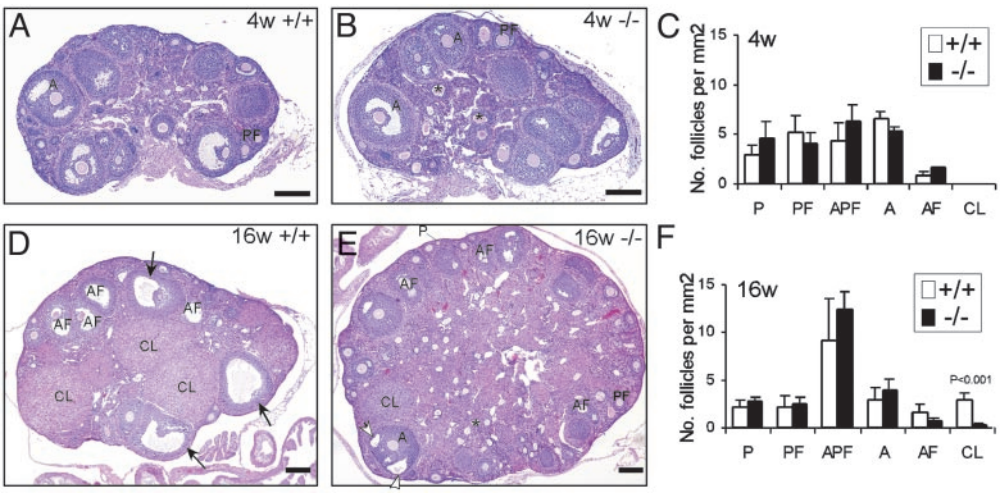

Fig. 2. Morphological comparison of ovaries from $AR^{+/+}$ and $AR^{-/-}$ females. (*A* and *B*) Ovaries from 4-week-old $AR^{+/+}$ and $AR^{-/-}$ females were histologically similar. (*C*) Statistical analysis of the number of the follicular compartments in $AR^{+/+}$ and $AR^{-/-}$ ovaries ($n = 2$). (*D* and *E*) The ovaries from sexually mature, 16-week-old $AR^{+/+}$ females, compared with their $AR^{-/-}$ counterparts. The granulosa layers in the antral follicles were locally thin (open arrowheads) in the $AR^{-/-}$ ovaries, whereas they were even in thickness in the $AR^{+/+}$ ovaries (arrows). An asterisk marks the zona pellucida remnants. (*F*) Statistical analysis of the number of the follicular compartments in $AR^{+/+}$ and $AR^{-/-}$ ovaries ($n = 3$ for each genotype). Statistical significance determined by using Student's unpaired and two-tailed *t* test is indicated. Representative sections are shown. P, primordial and primary follicle; PF, preantral follicle; APF, atretic primordial, primary, and preantral follicle; A, antral follicle; AF, atretic antral follicle; CL, corpus luteum. (Bar: 200 μm.)

BIOCHEMISTRY

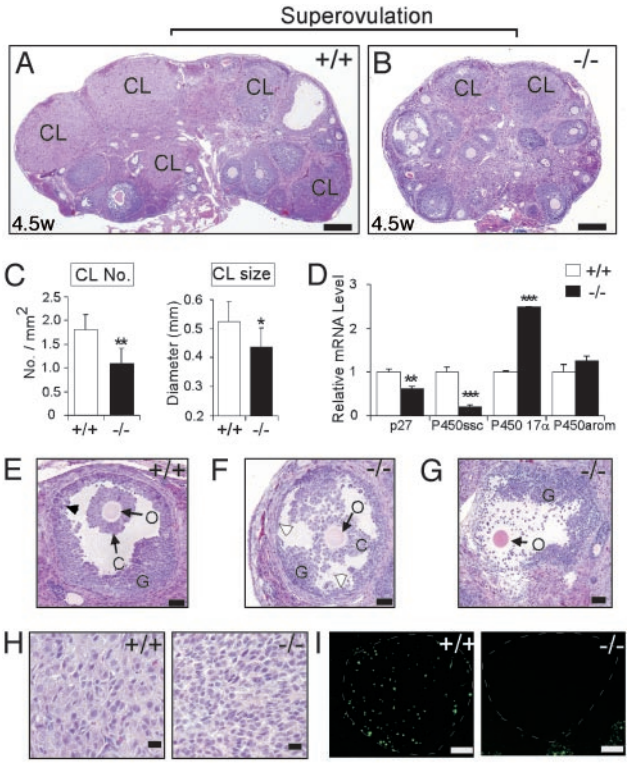

Fig. 3. Comparison of morphology and gene expression in ovaries of $AR^{+/+}$ and $AR^{-/-}$ females after superovulation treatment. Animals were injected with PMSG and then with hCG 48 h later and were killed after another 22 h. (*A* and *B*) Superovulated ovaries from 4.5-week-old $AR^{+/+}$ and $AR^{-/-}$ females ($n = 5$ for each genotype) were compared. Many CLs were induced by superovulation in the $AR^{+/+}$ ovaries, compared with fewer and smaller CLs in the $AR^{-/-}$ ovaries. (*C*) Statistical analysis of the number and size of CLs in both genotypes. *, $P < 0.05$; **, $P < 0.01$. (*D*) Real-time RT-PCR analysis of the expression levels of the functional markers for luteinization. Statistical significance determined by using Student's unpaired and two-tailed *t* test is indicated. **, $P < 0.01$; ***, $P < 0.001$. (*E* and *F*) Histological comparison at high magnification. In the $AR^{-/-}$ ovaries, the large antral follicles show decreased and disorganized granulosa cells, although the oocyte showed no sign of apoptosis. The granulosa layers were locally thin (open arrowhead) in the $AR^{-/-}$ ovaries, whereas they were even in thickness in the $AR^{+/+}$ ovaries (arrowhead). (*G*) The cumulus cells were disassociated from the oocyte during ovulation in the $AR^{-/-}$ ovaries. The possibility that this phenomenon may also occur in the $AR^{+/+}$ ovaries needs to be further investigated. O, oocyte; C, cumulus oophorus; G, granulosa cells. (*H*) The $AR^{+/+}$ CLs contain large lutea cells, whereas the $AR^{-/-}$ CLs contain early, small luteal cells, indicating delayed or impaired granulosa luteinization. (*I*) $AR^{+/+}$, but not $AR^{-/-}$, CLs (white dashed circles) show luteolysis (apoptosis) when TUNEL staining is used. Representative sections are shown. (Bars: *A* and *B*, 200 μm; *E–G*, 50 μm; *H*, 20 μm; *I*, 100 μm.)

ization (Fig. 3*I*), whereas those in $AR^{-/-}$ POFs only reached the small luteal cell stage, with no luteolysis (Fig. 3 *H* and *I*), implying that a delayed or impaired granulosa luteinization process occurs in $AR^{-/-}$ ovaries.

Determination of Apoptotic Cells in $AR^{-/-}$ Ovaries by Terminal Deoxynucleotidyltransferase-Mediated dUTP Nick End Labeling (TUNEL) Assay. To investigate whether the decrease of granulosa cells in the $AR^{-/-}$ POFs is a result of cellular apoptosis, TUNEL assays with *in situ* DNA labeling analyses were used on a wide spectrum of ovary sections. PMSG mimics the function of FSH to stimulate granulosa cell proliferation. When comparing ovaries after PMSG stimulation for 48 h, we found that the POFs in $AR^{-/-}$ ovaries could reach about the size of the $AR^{+/+}$ POFs but showed slight apoptotic signals (Fig. 4 *B* vs. *A*). After PMSG stimulation for 48 h, followed by hCG treatment for an additional 10 h to induce ovulation, many

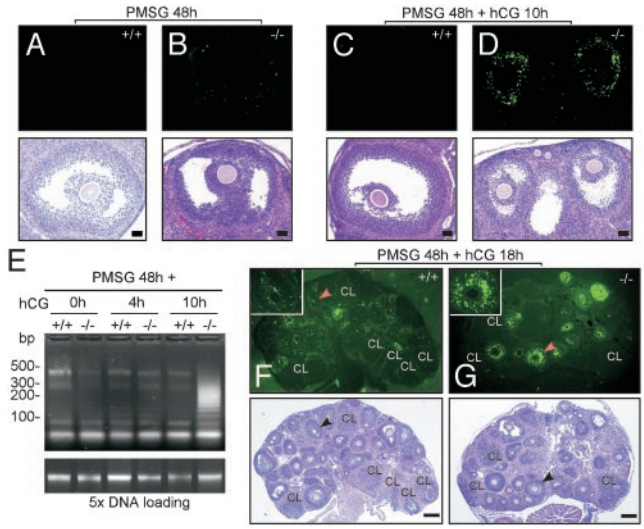

Fig. 4. Detection of apoptotic cells in the ovaries of $AR^{+/+}$ and $AR^{-/-}$ females treasted with exogenous gonadotropins by using TUNEL assay. The treatment conditions are as indicated. (*A* and *B*) Preovulatory follicles from both genotypes were compared. The $AR^{-/-}$ preovulatory follicle (*B*) shows slight apoptotic signals, whereas the $AR^{+/+}$ preovulatory follicle (*A*) shows no apoptosis. Note that after TUNEL staining and photographing (*Upper*), the sections were subjected to hematoxylin and eosin staining (*Lower*). (*C* and *D*) Preovulatory follicles during the periovulatory stage from both genotypes were compared. The $AR^{-/-}$ preovulatory follicle (*D*) shows intensive granulosa apoptosis and reduced size, whereas the $AR^{+/+}$ counterpart (*C*) shows no apoptosis. (*E*) The DNA fragmentation assay using ligation-mediated PCR. DNA ladders were amplified from 50 ng of genomic DNAs (*Upper*). At *Lower*, 250 ng of genomic DNAs (5×) is shown as loading control. (*F* and *G*) Superovulated ovaries from $AR^{+/+}$ and $AR^{-/-}$ females were compared. In the $AR^{+/+}$ ovaries, apoptotic granulosa cells were scattered in many follicles but not in CLs, whereas intensive granulosa apoptosis was seen in many preantral and antral follicles in the $AR^{-/-}$ ovaries. The *Inset* shows high magnification of the indicated follicles (arrowheads). Apoptotic signals are shown in bright green. Representative sections are shown. (Bar: *A–D*, 50 μm; *F* and *G*, 200 μm.)

POFs in the $AR^{-/-}$ ovaries apparently underwent granulosa cell apoptosis, resulting in reduced-size POFs, whereas the $AR^{+/+}$ POFs showed no apoptosis (Fig. 4 *D* vs. *C*). Consistently, a quantitative analysis of DNA fragmentation assays showed that the apoptotic extent was strongly increased in $AR^{-/-}$ ovaries, compared with their $AR^{+/+}$ counterparts, 10 h after hCG injection and after 48 h of PMSG treatment (Fig. 4*E*). When mice were treated with PMSG for 48 h and hCG for an additional 18 h, we observed intense apoptotic signals in many types of follicles, including primary, preantral, and antral follicles, in the $AR^{-/-}$ ovary (Fig. 4*G*), whereas the apoptotic granulosa cells were scattered in the $AR^{+/+}$ ovaries (Fig. 4*F*). Similar phenomena also occurred in the $AR^{-/-}$ ovaries that received PMSG for 48 h and hCG for an additional 22 h (data not shown). Together, these results suggest that AR may play an important role in granulosa cell survival during the periovulatory stage, and the absence of AR may cause granulosa cells to be more susceptible to apoptosis.

Comparison of Gene Expressions Between $AR^{+/+}$ and $AR^{-/-}$ Ovaries. The gene expression was quantitated by using real-time RT-PCR on the RNAs extracted from whole ovaries. To evaluate the AR role in primordial and primary follicles, we used the ovaries from 10-day-old mice (Fig. 5*A*). We found that FSH receptor (FSHR) expression is markedly reduced in the $AR^{-/-}$ ovaries, compared with their $AR^{+/+}$ counterparts. The expression level of insulin-like growth factor-I receptor is also reduced in the $AR^{-/-}$ ovaries, but to a lessened extent. When comparing 4.5-week-old ovaries treated with PMSG for 48 h with or without hCG for an additional 10 h,

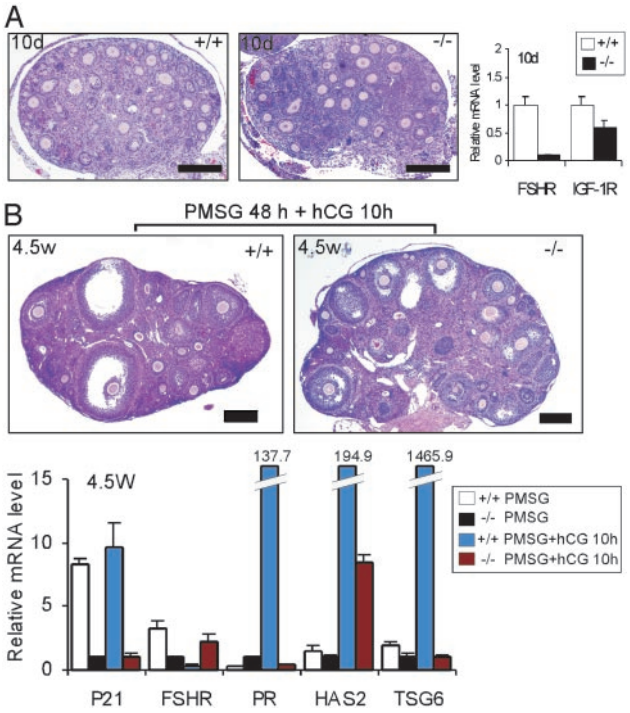

Fig. 5. Real-time RT-PCR analysis for gene expression. Whereas one ovary was processed for histological examination, the other one from the same mouse was subjected to real-time RT-PCR. (*A*) Comparison of ovarian morphology between $AR^{+/+}$ and $AR^{-/-}$ mice ($n = 2$ for each genotype) at 10 days of age. The expression levels of FSHR and insulin-like growth factor-I receptor mRNA were quantitated by using real-time RT-PCR. (*B*) Comparison of ovarian morphology between $AR^{+/+}$ and $AR^{-/-}$ mice at 4.5 weeks of age. The conditions of exogenous gonadotropin treatments were as indicated. The expression levels of indicated genes were quantitated by using real-time RT-PCR. FSHR, follicle-stimulating hormone receptor; IGF-IR, insulin-like growth factor-I receptor; PR, progesterone receptor; HAS2, hyaluronan synthase 2; TSG6, tumor necrosis factor-α-stimulated gene 6. (Bar: *A*, 50 μm; *B*, 200 μm.)

we found that the expression level of p21, which is known to be essential for granulosa luteinization (20), is very low in the $AR^{-/-}$ ovaries (Fig. 5*B*). In addition, consistent with the result from the 10-day-old $AR^{-/-}$ ovaries (Fig. 5*A*), FSHR expression remained low in the $AR^{-/-}$ ovaries that received PMSG for 48 h. In agreement with ref. 21, which demonstrates that FSHR expression is diminished after the LH surge, we also found that FSHR expression is reduced at 10 h after hCG administration in the $AR^{+/+}$ ovaries, whereas FSHR expression is unexpectedly increased in the $AR^{-/-}$ ovaries. Progesterone signaling is important for protecting POFs from atresia during granulosa luteinization, in conjunction with the induction of progesterone receptors shortly after the LH surge (22). Therefore, the much lower induction of progesterone receptors in $AR^{-/-}$ ovaries at 10 h after hCG injection causing the dampened progesterone signaling may lead to granulosa cell apoptosis (Fig. 5*B*). Hyaluronan synthase 2 and tumor necrosis factor-α-stimulated gene 6, which are highly induced after the LH surge and are involved in the cumulus cell expansion (23), were also markedly reduced in $AR^{-/-}$ ovaries (Fig. 5*B*), which may result in the poor development of COCs.

Uterine Response of Female $AR^{-/-}$ Mice to Superovulation. We also examined the uterine function of $AR^{-/-}$ and $AR^{+/+}$ mice. The uteri of $AR^{-/-}$ mice develop normally and possess histologically normal compartments. However, the diameters of uteri in female $AR^{-/-}$ mice were smaller than those in $AR^{+/+}$ mice (Fig. 1*C*). After superovulation treatment, the difference became more significant (Fig. 6*A*). The uterine wall, consisting of the smooth muscle layer,

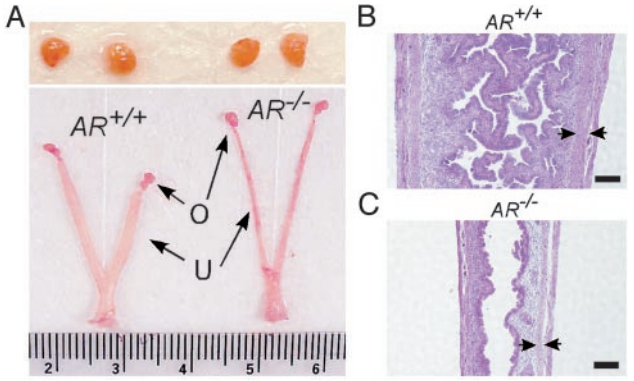

Fig. 6. Comparison of uterine response to superovulation treatment in 4.5-week-old $AR^{+/+}$ and $AR^{-/-}$ females. (*A*) Comparison of ovary size in both genotypes (*Upper*). The $AR^{+/+}$ uteri were wider in diameter and showed apparent thicker uterine walls, whereas $AR^{-/-}$ uteri did not respond properly (*Lower*). O, ovary; U, uterus. (*B* and *C*) Comparison of longitudinal sections shows that $AR^{+/+}$ (*B*), but not $AR^{-/-}$ (*C*) uteri showed the luteal response, as evident by the massive uterine hypertrophy and endometrial growth. The double arrowheads show the diameter of the muscular layer. (Bar: 200 μm.)

was also decreased in $AR^{-/-}$ mice (Fig. 6 *C* vs. *B*). In contrast to $AR^{-/-}$ uteri, the $AR^{+/+}$ uteri showed apparent uterine hypertrophy and endometrial growth in response to exogenous gonadotropins (Fig. 6 *B* vs. *C*). Consistent with the phenomenon, the uterine weights were 90.6 ± 16.8 and 38.6 ± 14.9 mg in $AR^{+/+}$ and $AR^{-/-}$ mice, respectively, after PMSG treatment for 48 h ($n = 2$ for each genotype). Also, the uterine weights were 105.2 ± 15.4 and 37.3 ± 27.4 mg in $AR^{+/+}$ and $AR^{-/-}$ mice, respectively, after receiving PMSG for 48 h and hCG for an additional 4 h ($AR^{+/+}, n = 3; AR^{-/-}$, $n = 2$; $P = 0.034$). It is noteworthy that, under the same conditions, there is no significant difference in the ovarian weights of $AR^{+/+}$ and $AR^{-/-}$ mice (data not shown).

Discussion

The Important Role of the AR in Folliculogenesis. Using the Cre-lox system, we have generated female mice homozygously lacking AR and have provided *in vivo* evidence of AR roles in female physiology. The gross examination of female $AR^{-/-}$ mice appeared normal; however, the continuous mating study illuminates the subfertility of female $AR^{-/-}$ mice. To understand the mechanisms underlying the reduced fertility in female $AR^{-/-}$ mice, we investigated the phenotype of the $AR^{-/-}$ ovary. The ovarian development in $AR^{-/-}$ females is normal before puberty. However, at maturity, the $AR^{-/-}$ ovary exhibits a marked reduction in follicular maturation, as evidenced by fewer CLs in the ovaries (Fig. 2). After treatment with exogenous gonadotropins, which bypasses the influence of the hypothalamus–pituitary axis, the $AR^{-/-}$ females produced fewer oocytes (Table 2) and showed a significant decrease in CL formation and a prominent granulosa apoptosis event in the ovaries (Figs. 3 and 4), thereby suggesting that the AR plays an important role in ovarian folliculogenesis. In addition, as female $AR^{-/-}$ mice show significantly longer estrous cycles, which correlates well with the reduced litter numbers (Table 1), possible defects in the hypothalamus–pituitary axis and other neuroendocrine pathways may exist.

Cell apoptosis occurs in all stages of follicular development, mainly in the early antral follicles. Compared with the follicles at earlier stages, POFs protected by redundant signaling pathways are much less susceptible to apoptosis to ensure subsequent ovulation (9). Interestingly, our studies on $AR^{-/-}$ ovarian morphology have shown that intensive granulosa apoptosis occurs in the POFs 10 h after hCG injection after PMSG administration for 48 h (Fig. 4). hCG, which mimics the function of LH, triggers the differentiation of granulosa cells into cumulus cells and

luteal cells, which involves the transition from cell proliferation to growth arrest and is concurrent with down-regulation of cyclin D2 and up-regulation of p27 and p21 gene expression (20). The marked reduction of p21 expression in the $AR^{-/-}$ ovary at this stage (Fig. 5*B*) may disturb the process of terminating proliferation, leading to cell apoptosis. p21 is one of the AR target genes, and its promoter region contains an androgen response element located 200 bp upstream of the transcriptional initiation site (24). Therefore, it is conceivable that p21 expression may be regulated by AR during the periovulatory stage.

Although apparent cell apoptosis could be detected in the $AR^{-/-}$ POFs, whether the apoptosis level is increased in the follicles at the earlier stages needs to be further investigated. Nevertheless, a marked decrease in FSHR expression in the ovaries from 10-day-old $AR^{-/-}$ mice as well as from 4.5-week-old PMSG-primed $AR^{-/-}$ mice supports the previous findings that androgen treatment enhances FSHR expression and that AR expression is associated with follicular proliferation (25, 26). Also, the important role of AR in the early stages of follicular growth is elucidated by the *in vitro* follicle culture experiment that showed that the cultured follicles fail to develop to POFs when AR activity is inhibited by antiandrogen treatment (27).

Intensive granulosa cell apoptosis in the POFs of the $AR^{-/-}$ ovaries also impairs the differentiation of granulosa cells into cumulus cells. At least three lines of evidence show the poor development of COCs in the $AR^{-/-}$ ovary: (*i*) the genes required for cumulus cell expansion, such as hyaluronan synthase 2 and tumor necrosis factor-α-stimulated gene 6 (23), are dramatically reduced in the $AR^{-/-}$ ovary; (*ii*) cumulus cells were more quickly disassociated from the oocytes collected from the gonadotropin-primed $AR^{-/-}$ mice after hyaluronidase digestion; and (*iii*) cumulus cells are mostly disassociated from oocytes in some of the POFs during ovulation. Therefore, the poor quality of COCs implies the lower fertilization rate of the $AR^{-/-}$ oocytes, resulting in the reduced fertility of $AR^{-/-}$ mice.

The reduced size of the CLs in the $AR^{-/-}$ ovary suggests that the number of granulosa cells is decreased. It has been known that a certain number of granulosa cells must be present in the ovary for ovulation to occur (20). Therefore, the reduced number of CLs in the $AR^{-/-}$ ovaries could be in part due to the much lower number of granulosa cells in some of the POFs, which results in a reduction of ovulation events (Table 1) and a subsequent reduction in CL formation. Nevertheless, we could not rule out the possibility that low CL numbers in the $AR^{-/-}$ ovaries result from fewer follicles that can reach the POF stage, the stage that precedes ovulation.

A few female $AR^{-/-}$ mice were infertile at 5–6 months of age. Whether this early termination of the breeding capacity is directly due to the loss of functional AR may need more intensive studies with many more mice and longer trial times. However, it may involve the premature ovarian failure linked to the exhaustion of the reserved primordial follicles. All primordial follicles initiated to grow are programmed to undergo apoptosis unless rescued by FSH or other survival factors (9, 28, 29). Presumably, the original number of primordial follicles reserved is similar in $AR^{+/+}$ and $AR^{-/-}$ mice. However, the lack of CL formation in female $AR^{-/-}$ mice may increase follicle recruitment and, together with increasing follicular atresia, may result in the early exhaustion of the primordial follicles, reduction of the reproductive life span, and earlier termination of breeding capacity.

Impaired Uterine Response to Gonadotropins in Female $AR^{-/-}$ Mice. An early study indicated that androgens could increase uterine weight in rats (30). In female $AR^{+/+}$ mice, the superovulation stimulation shows an increase in the size of the uterus, with a typical change of uterine hypertrophy and endometrial growth required for implantation (31). In contrast, the cellular transformation in the $AR^{-/-}$ uteri was obviously reduced (Fig. 6). Moreover, an increase in the size of the placenta (placentamegaly) is commonly found in pregnant $AR^{-/-}$ mice (data not shown), which may be a compensation of the defective uteri for maintaining adequate nutrition and/or oxygenation for embryo growth.

The progesterone levels were reduced in $AR^{-/-}$ females (by up to 50% of levels found in their $AR^{+/+}$ counterparts) (7). This is likely due to the formation of fewer and smaller CLs in $AR^{-/-}$ ovaries in conjunction with the low expression of CL-specific side-chain cleavage cytochrome P450, an enzyme required for progesterone production. Those characteristics fit the clinical disorder "luteal phase defect," which is associated with reduced progesterone production in women. Luteal phase defect is a common endocrine disorder associated with infertility and spontaneous miscarriage and is found in 3–10% of the female population (32). The causes of this disease include defective follicular maturation, a suboptimal preovulatory gonadotropin surge, and/or reduced luteotropic support. Therefore, the loss of AR in female mice that develop luteal phase defect-like symptoms may suggest that this disorder can be caused by insufficient AR activity.

In summary, female $AR^{-/-}$ mice exhibit reduced fertility with defective folliculogenesis, reduced CL formation, and reduced uterine response to gonadotropins. The discovery that AR plays an important role in granulosa cell development and is required for the optimal performance of female reproduction may help obstetricians/gynecologists to further diagnose and/or treat many female patients.

We thank Karen Wolf for help with manuscript preparation. This work was supported by National Institutes of Health Grants DK60905 and DK60948 and the George H. Whipple Professorship Endowment.

1. Heinlein, C. A. & Chang, C. (2002) *Endocr. Rev.* **23,** 175–200.
2. Heinlein, C. A. & Chang, C. (2004) *Endocr. Rev.* **25,** 276–308.
3. Chang, C. S., Kokontis, J. & Liao, S. T. (1988) *Science* **240,** 324–326.
4. Yeh, S., Hu, Y. C., Rahman, M., Lin, H. K., Hsu, C. L., Ting, H. J., Kang, H. Y. & Chang, C. (2000) *Proc. Natl. Acad. Sci. USA* **97,** 11256–11261.
5. Yeh, S., Lin, H. K., Kang, H. Y., Thin, T. H., Lin, M. F. & Chang, C. (1999) *Proc. Natl. Acad. Sci. USA* **96,** 5458–5463.
6. Chang, C., Chen, Y., Yeh, S. D., Xu, Q., Wang, R.-S., Guillou, F., Lardy, H. & Yeh, S. (2004) *Proc. Natl. Acad. Sci. USA* **101,** 6876–6881.
7. Yeh, S., Hu, Y. C., Wang, P. H., Xie, C., Xu, Q., Tsai, M. Y., Dong, Z., Wang, R. S., Lee, T. H. & Chang, C. (2003) *J. Exp. Med.* **198,** 1899–1908.
8. Murphy, B. D. (2000) *Biol. Reprod.* **63,** 2–11.
9. McGee, E. A. & Hsueh, A. J. (2000) *Endocr. Rev.* **21,** 200–214.
10. Horie, K., Takakura, K., Fujiwara, H., Suginami, H., Liao, S. & Mori, T. (1992) *Hum. Reprod.* **7,** 184–190.
11. Wang, H., Andoh, K., Hagiwara, H., Xiaowei, L., Kikuchi, N., Abe, Y., Yamada, K., Fatima, R. & Mizunuma, H. (2001) *Endocrinology* **142,** 4930–4936.
12. Vendola, K., Zhou, J., Wang, J., Famuyiwa, O. A., Bievre, M. & Bondy, C. A. (1999) *Biol. Reprod.* **61,** 353–357.
13. Daniel, S. A. & Armstrong, D. T. (1980) *Endocrinology* **107,** 1027–1033.
14. Billig, H., Furuta, I. & Hsueh, A. J. (1993) *Endocrinology* **133,** 2204–2212.
15. Cheng, G., Weihua, Z., Makinen, S., Makela, S., Saji, S., Warner, M., Gustafsson, J. A. & Hovatta, O. (2002) *Biol. Reprod.* **66,** 77–84.
16. Yeh, S., Tsai, M. Y., Xu, Q., Mu, X. M., Lardy, H., Huang, K. E., Lin, H., Yeh, S. D., Altuwaijri, S., Zhou, X., *et al.* (2002) *Proc. Natl. Acad. Sci. USA* **99,** 13498–13503.
17. Ikeda, S., Imai, H. & Yamada, M. (2003) *Reproduction* **125,** 369–376.
18. Zaczek, D., Hammond, J., Suen, L., Wandji, S., Service, D., Bartke, A., Chandrashekar, V., Coschigano, K. & Kopchick, J. (2002) *Biol. Reprod.* **67,** 1115–1124.
19. Lyon, M. F. & Glenister, P. H. (1980) *Proc. R. Soc. London Ser. B* **208,** 1–12.
20. Robker, R. L. & Richards, J. S. (1998) *Mol. Endocrinol.* **12,** 924–940.
21. Yaron, Y., Schwartz, D., Evans, M. I., Lessing, J. B. & Rotter, V. (1998) *J. Reprod. Med.* **43,** 435–438.
22. Peluso, J. J. & Pappalardo, A. (1998) *Biol. Reprod.* **58,** 1131–1137.
23. Ochsner, S. A., Day, A. J., Rugg, M. S., Breyer, R. M., Gomer, R. H. & Richards, J. S. (2003) *Endocrinology* **144,** 4376–4384.
24. Lu, S., Liu, M., Epner, D. E., Tsai, S. Y. & Tsai, M. J. (1999) *Mol. Endocrinol.* **13,** 376–384.
25. Weil, S., Vendola, K., Zhou, J. & Bondy, C. A. (1999) *J. Clin. Endocrinol. Metab.* **84,** 2951–2956.
26. Weil, S. J., Vendola, K., Zhou, J., Adesanya, O. O., Wang, J., Okafor, J. & Bondy, C. A. (1998) *J. Clin. Endocrinol. Metab.* **83,** 2479–2485.
27. Murray, A. A., Gosden, R. G., Allison, V. & Spears, N. (1998) *J. Reprod. Fertil.* **113,** 27–33.
28. Hsueh, A. J., Eisenhauer, K., Chun, S. Y., Hsu, S. Y. & Billig, H. (1996) *Recent Prog. Horm. Res.* **51,** 433–455; discussion 455–456.
29. Durlinger, A. L., Visser, J. A. & Themmen, A. P. (2002) *Reproduction* **124,** 601–609.
30. Armstrong, D. T. & Papkoff, H. (1976) *Endocrinology* **99,** 1144–1151.
31. Paria, B. C., Reese, J., Das, S. K. & Dey, S. K. (2002) *Science* **296,** 2185–2188.
32. Insler, V. (1992) *Curr. Opin. Obstet. Gynecol.* **4,** 203–211.